Nanoscale

PAPER

View Article Online
View Journal

Cite this: DOI: 10.1039/d5nr01087j

Understanding structure–property relationships in coordination polymers: a comparative study of the copper(II) and zinc(II) coordination mechanism†

Vasiliki Benekou,[a] Zhe Zhang,[b] Lukas Sporrer,[b] Andrea Candini,[a] Filippo Monti,[a] Alessandro Kovtun,[a] Fabiola Liscio,[c] Stefan C. B. Mannsfeld,[b] Xinliang Feng,[b] Renhao Dong[d,e] and Vincenzo Palermo *[a,f]

Coordination polymers (CPs) are an interesting class of materials due to their tunable structures and electrical properties where, however, the correlation between the former and latter is still not fully understood. Here we compare the structures and properties of CPs derived from copper(II) and zinc(II) ions coordinating a triphenylene derivative (OHPTP). To focus on the effect of the coordinating ion used and avoid possible differences due to the processing method, we synthesized different CPs using a novel two-step technique, potentially scalable for applications in transistors, sensors, and photovoltaics: first, the organic ligand is deposited using a shear-coating technique which ensures uniform deposition on the macroscopic scale. Then, in the second step, the sample is exposed to solutions of the metal ions, which can penetrate in the organic layer to coordinate with the ligand. Density functional theory (DFT) calculations show that Cu ions have a higher affinity for the ligand and form square-planar CP structures due to their d^9 electronic configuration. Conversely, Zn ions can coordinate with the chelating ligands using only their empty 4s and 4p orbitals to achieve sp^3 hybridisation, thus preferring to adopt a tetrahedral geometry and leading to less ordered structures with significantly hampered conductivity. FT-IR and UV-vis spectra, XPS and conductive atomic force microscopy confirm the distinct coordination behaviour of Cu and Zn ions. Thermal stability analysis further shows that Zn-based CPs retain their structural integrity at temperatures up to 300 °C, whereas Cu-based CPs degrade earlier. These results show how metal–ligand interactions impact the properties of CPs, enhancing the understanding of structure–property relationships, and provide practical insights for designing CPs with desired electronic and thermal properties by varying the coordinating metal ions.

Received 14th March 2025,
Accepted 15th May 2025

DOI: 10.1039/d5nr01087j

rsc.li/nanoscale

1. Introduction

Significant progress has been recently made in the field of molecular inorganic–organic hybrid compounds with the synthesis and characterization of large networks in one, two, and three dimensions (1D, 2D, and 3D). In particular, attention has been paid to coordination compounds with almost infinite periodic structures where organic building blocks act as ligands and metal ions as nodes to form networks.[1–4] These compounds are typically termed coordination polymers (CPs).[1,5,6] Typically, both the structures of organic ligands and the coordination geometries of metal ions are diverse.[3] The arrangements of various metal ions (or clusters) and organic bridging ligands can form extended coordination structures,[7] showcasing a wide variety of resulting final configurations.

Coordination polymers have attracted commercial interest as promising options for gas separation and storage applications because of their porosity, which enables the adsorption and storage of gases like carbon dioxide and hydrogen. Additionally, one noteworthy feature of coordination polymers that results from the selection of metal ions and organic

[a]Institute for Organic Synthesis and Photoreactivity, National Research Council of Italy, Via Gobetti 101, Bologna, Italy. E-mail: vincenzo.palermo@cnr.it
[b]Chair of Molecular Functional Materials, Faculty of Chemistry and Food Chemistry Technische Universität Dresden, Mommsenstrasse 4, Dresden 01062, Germany
[c]Institute of Nanostructured Materials, National Research Council of Italy, Via Gobetti 101, Bologna, Italy
[d]Department of Chemistry, The University of Hong Kong, Hong Kong 999077, China
[e]Materials Innovation Institute for Life Sciences and Energy (MILES), HKU-SIRI, Shenzhen 518048, China
[f]Department of Industrial and Materials Science, Chalmers University of Technology, SE-412 96 Göteborg, Sweden

†Electronic supplementary information (ESI) available. See DOI: https://doi.org/10.1039/d5nr01087j

ligands is the tunability of their properties. Researchers can control the coordination polymer's size, shape, and functionality by altering the constituents, resulting in a large library of materials with customized properties. The formation of coordination networks and their various forms, such as bulk crystals, polycrystalline films, and amorphous films, can be influenced by a wide range of synthetic processes and reaction parameters, including pH, solvent, reaction/crystallization temperature, template/additive, and counter ions.[8]

CPs with useful electronic properties can be formed by redox-driven coordination polymerization reactions of suitable organic conjugated ligands featuring adjacent dihydroxy, diamino, or dithiol functionalities with metal ions, forming 2D d–π conjugated planes. Key properties of such structures are due to their planar MX_4 bonds (*e.g.*, CuO_4 structures, Fig. 1a and b). For a recent review, see ref. 9.

Changing the metal used for bonding will cause profound changes in the CP structure. As a testbed example, we consider Cu^{2+} and Zn^{2+} ions, both of which can be used to produce CPs. These ions have a similar size (0.72 Å and 0.74 Å, respectively)[10] and are close neighbours in the periodic table, but the difference of one electron in their electronic configuration can provide significantly different coordination behaviours. The Cu^{2+} ion yields planar CP structures because it features a d orbital partially-empty ($[Ar]3d^9$), forming square-planar 4-coordinate compounds thanks to its dsp^2 hybridization with two *ortho*-dihydroxyl functional groups using 3d, one 4s, and two 4p orbitals (Fig. 1c). The electronic configuration of Zn^{2+} ions, instead, features its d orbitals completely filled ($[Ar]3d^{10}$), leading to tetrahedral 4-coordinate compounds having sp^3 hybridization with the dihydroxyl functional groups using only its empty 4s and 4p orbitals.

It can thus be predicted that CPs obtained using Cu and Zn ions will have similar stoichiometry but deeply different structures, with the Cu CP being planar and the Zn CP being more disordered.

Here, we will study the structural and electronic properties as well as the thermal stability of two CPs prepared with the same organic ligand and synthesis procedure but using Cu and Zn ions.

As a test model, we used an organic ligand named 2,3,6,7,11,12,15,16-octahydroxyphenanthro[9,10:*b*]triphenylene (OHPTP), which was used recently combined with Cu ions to produce a p-type semiconductor CP with interesting properties: a near IR band gap of about 0.50 eV, a high electrical conductance of 0.10 S cm^{-1} and a high charge carrier mobility of approx. 10.0 $cm^2\ V^{-1}\ s^{-1}$.[11] Computational studies suggest that the electrical properties of such Cu-based CPs are due to the out-of-plane interactions of their stacked ligands. Thus, changing the Cu ions with Zn ions, less favourable for providing planar MX_4 bonds, would radically change some of these properties.

Coordination polymers can be created using a variety of techniques, from conventional solution-based methods to more advanced techniques like solvothermal and mechanochemical synthesis, and the final structure of the CPs depends not only on the ligand and metal, but also on the processing conditions. To focus on the effect of the coordinating ion used and avoid possible differences due to the processing method, we synthesized different CPs using the same method. Specifically, we adopted a novel two-step technique (Fig. 2), where the organic ligand is first deposited using shear-coating; then, in the second step, the organic layer is exposed to solutions of different ions, which can penetrate the organic layer to coordinate with the ligand.

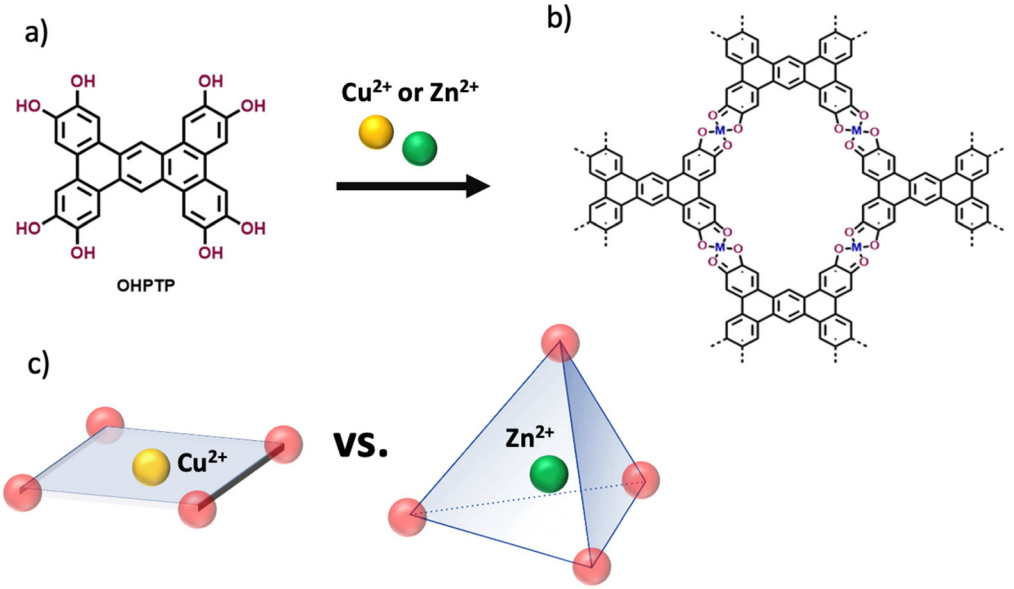

Fig. 1 (a) Structure of the OHPTP organic ligand used. (b) Idealized structure of the CP formed by the reaction of the organic ligand and metallic Cu or Zn ions. (c) Schematic representation of possible square planar or tetrahedral coordination structures favoured by different ions with four oxygen atoms.

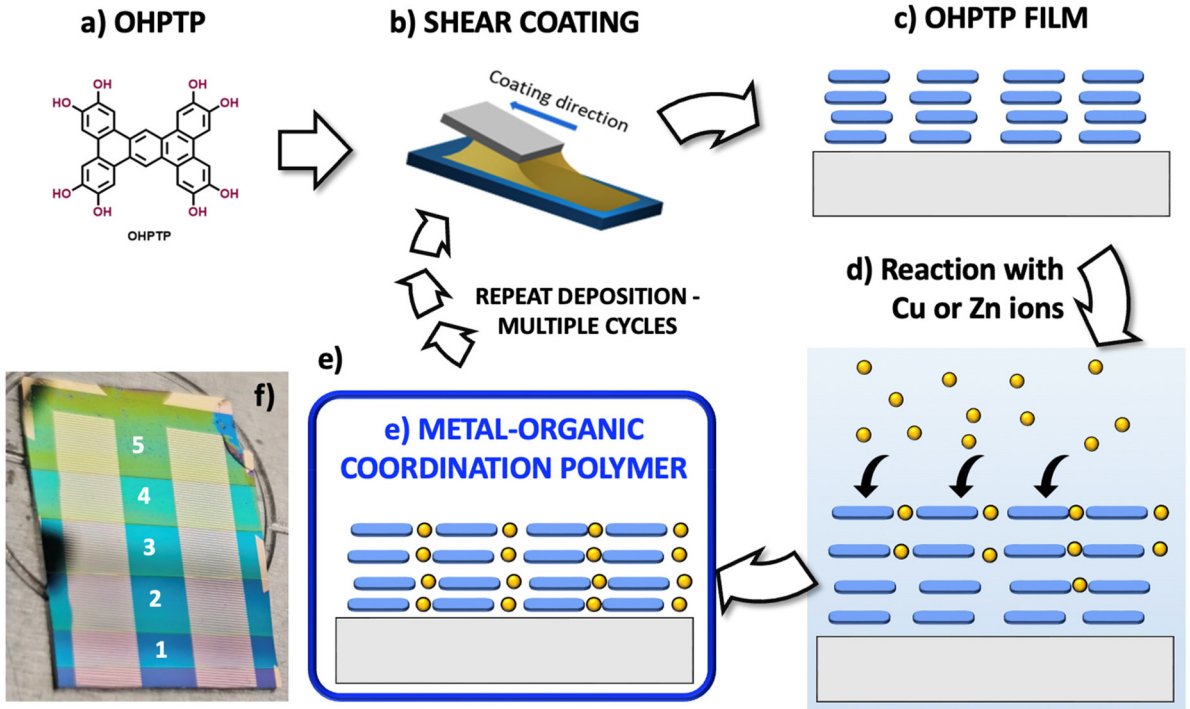

Fig. 2 Scheme of the two-step procedure used to create the CP. (a) The organic building block OHPTP. (b) Shear coating of the organic molecules to obtain a uniform film (c), which is then dipped in a solution of Cu or Zn ions (d) to obtain the CP (e). (f) Photograph of a sample with uniform coatings obtained by multiple shear coating + dipping cycles; the white numbers indicate the number of cycles.

The shear-coating method is a type of meniscus-guided coating known for low-cost and high-throughput thin-film fabrication.[12–17] In the shear-coating technique, the organic material to be deposited is confined between a top movable blade and a temperature-controlled substrate.[13,14,16–21] The material is spread across the substrate by shifting the blade at a set speed, resulting in a guided and regulated film deposition. Shear coating parameters, including stage temperature, blade gap and speed, can affect the films' properties.[13] In addition, a variety of well-established techniques exist for regulating the final film morphology. These include pre-processing methods for ink formulation, alignment methods for post-processing, substrate patterning, and modified shear coating geometry methods.[18] Numerous variables, including the substrate's surface energy, solution concentration and viscosity, shearing speed, and substrate temperature, affect the final morphology of the deposited material.[19]

Shear coating is a versatile and easy method for achieving uniformity, good molecular arrangement, and stacking in films with the least amount of material waste. In this way, we rule out possible differences of morphology due to the initial deposition of the ligand (the first step of fabrication). This approach provides greater versatility than the usual organic metal assembly from bulk solutions; furthermore, shear coating can be applied on large areas, making it viable also for practical industrial applications to produce transistors, sensors, and photovoltaics. We prepared samples by varying the reaction time of the as-deposited ligand when immersed in the metal ion solution, with reaction times ranging from 1 to 20 minutes. The thickness of the films was adjusted by repeating the deposition–reaction procedure for multiple cycles (Fig. S1–S3†). The two classes of CP materials prepared with Cu and Zn with different reaction times and numbers of cycles were then compared using microscopic, spectroscopic, and electrical characterization techniques, as detailed below.

2. Results and discussion

Preparation of CP thin films using the shear coating technique

The OHPTP monomer (Fig. 1a) used to prepare the CP films under study was synthesized as described previously.[11] In the first step of the process, a blend of the OHPTP monomer was dissolved in THF with a concentration of 0.004 M and sheared on an Au/Si substrate at 35 °C (Fig. 2). During the shear-coating process, the gap between the blade and the substrate was fixed at a distance of 250 μm and the speed of the coating process was 6 mm s^{-1}. Then, in the second step of the procedure, the sample was dipped into a solution containing the second component of the CP, *i.e.*, the metal ion. Water solutions of Cu $(OAc)_2$ or $Zn(NO_3)_2$ were used for different reaction times to form the coordination polymer. The films were stable in water. We prepared four separate samples for each of the two reactants, with varying reaction/dipping times, with t = 5, 10, 15 or 20 minutes.

Several studies in the literature have examined ion diffusion in thin layers of triphenylene derivatives.[22–26] Due to the open, nanoporous structure characteristic of these materials, ion diffusion is typically very rapid; the OHPTP molecule described here, even in its pristine form, is expected to form an open crystalline structure with pores even larger than those in conventional triphenylenes.

Furthermore, the shear coating technique could be applied multiple times on the same substrate; this allowed us to realize samples covered by multiple CP layers. Fig. 2 shows the process of each coating and how multiple coatings were produced. For this study, we realized two samples, one for each of the reactants, repeating the coatings six times. Fig. S1 in the ESI† shows photographs of samples with single and multiple coatings. Fig. S2† shows the AFM characterization of multi-coated samples and the relative thickness of each coating, with the presence of some aggregates and voids on the surface, which anyhow could be attributed to dust or impurities always present in samples prepared under a standard atmosphere outside a clean room. We performed SEM/energy-dispersive spectroscopy (EDS) characterization on the samples, which showed a uniform distribution of metals in the layer (Fig. S3†).

For the sake of comparison, we also prepared bulk samples of the Cu and Zn CPs, obtained by a one-step procedure with simple mixing of the two reactants in solution. To this aim, the direct reaction of OHPTP and copper acetate (in the case of the Cu_2OHPTP crystal) and zinc nitrate (in the case of the Zn_2OHPTP crystal) was performed in a solvent mixture of water and DMF (7 : 3) at 85 °C for 24 hours.[11]

Characterization of the CP thin films

All CP samples were characterised by X-ray photoemission spectroscopy (XPS), Fourier-transform infrared (FT-IR) spectroscopy and UV-vis spectroscopy. X-ray photoemission spectroscopy (XPS, Fig. 3) was used to confirm that the CPs contained only the elements composing the ligand (C and O) and each of the two metal ions (Cu and Zn, respectively), and it provided the ratio of the number of atoms present in each element (Table 1): Cu CP samples contained only copper and no other metal ions, while Zn CP samples contained only zinc, confirming that the only ions in the material were the ones

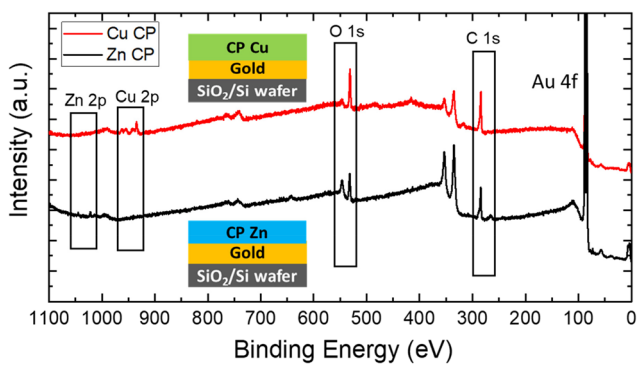

Fig. 3 XPS spectra of the Cu CP and Zn CP materials.

Table 1 Atomic ratios of the main elements for different ion–ligand reaction times for the single-coated Cu and Zn films (formation time of the coordination polymer)

Atom% (XPS)	C	D	Zn	Cu	Ion/ligand ratio (ideal = 2)
Cu CP 1 min	61.5	22.8	—	**1.6**	0.78
Cu CP 20 min	64.9	25.8	—	**3.1**	1.43
Zn CP 1 min	46.9	18.7	**0.4**	—	0.26
Zn CP 20 min	50.2	18.8	**0.9**	—	0.54

introduced during the reaction stages with $Cu(OAc)_2$ or $Zn(NO_3)_2$ solutions, respectively.

In Cu CP samples, high-resolution XPS spectra of O 1s show a broad peak that may be attributed to a combination of C═O–Cu (531 eV) and C–O–Cu (532 eV) signals and the contribution of water (Fig. S4†). Zn CP samples also exhibit the same contributions in the O 1s signal as Cu CP samples (Fig. S5†), but with Zn in place of Cu. The C 1s signal of both types of films, showing three main peaks at 284.5 eV, 286.4 eV and 288.3 eV, is attributed to C═C, C–O, and C═O, respectively. In the energy range typical for Cu 2p, a peak at 934.6 eV suggests the presence of Cu(II), while the faint signal observed at 932.5 eV and usually assigned to Cu(I) is attributed to the partial reduction of Cu(II) due to X-ray irradiation during the XPS measurement, with some C–OH groups oxidizing to C═O.[27,28] Finally, the presence of Zn is deduced from the Zn 2p signals at 1022 eV and 1045 eV.

Table 1 displays the abundance ratios of the main elements in each of the single-coated Cu and Zn CP samples for two distinct reaction times (1 and 20 minutes) extracted from the XPS spectra, reported as atom percentages. The signal of gold is also recorded, resulting from the substrate (not shown in the table). The atomic abundance of metal ions/ligands in the materials increases with dipping time but never reaches the theoretical stoichiometric limit for such CPs (the ideal ratio equals 2), *i.e.*, M_2OHPTP. Cu ions penetrated more effectively than Zn ions in the sample, reaching an ion/ligand ratio of 1.43 after 20 min of reaction time; Zn ions reached a much lower ratio of 0.9 for the same reaction time, indicating a less favourable interaction with the ligand.

Fourier-transform infrared (FT-IR) spectroscopy confirmed that ions and ligands do react with each other, with the formation of coordination bonds (Fig. 4a). The O–H stretching vibration band of OHPTP at 3000–3500 cm^{-1} decreased after the complexation of the ligand film with Cu-OHPTP and Zn-OHPTP.

We compared the thin films of Cu CP and Zn CP prepared *via* shear coating with the bulk crystals of the corresponding materials prepared *via* solvothermal synthesis.[12] Fig. S6† shows the comparison of the IR spectra of the standard, bulk Cu and Zn CPs prepared from solution, which are significantly different from those of the thin films obtained by on-surface synthesis, as the main bands are either missing or shifted. For instance, the crystals obtained in bulk solutions show complete coordination of the OH group since the spectra lack the

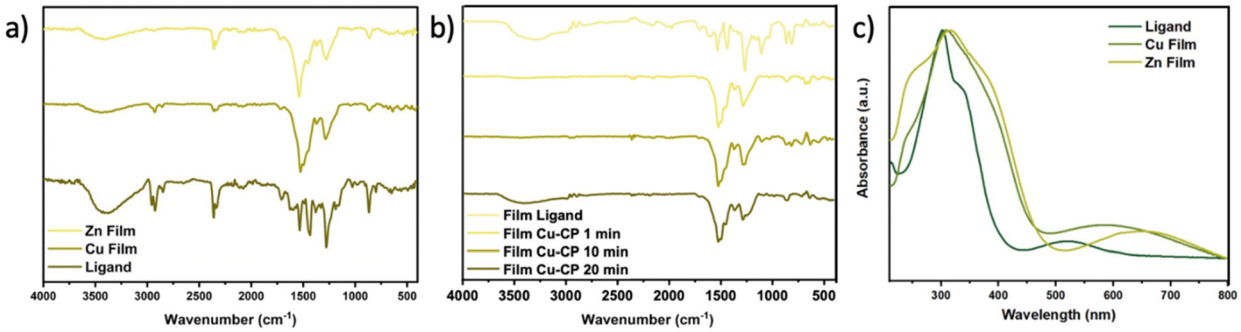

Fig. 4 (a) IR spectra of the ligand, Cu CP film and Zn CP film, (b) IR spectra of the Cu CP films at different reaction times and the ligand and (c) UV/vis spectra of the ligand, Zn CP film and Cu CP film.

characteristic band of the O–H stretching vibration at 3000–35 000, but the thin films still exhibit this band, suggesting incomplete coordination, as well as the presence of water.

UV-visible spectroscopy provides additional confirmation of the formation of the polymer. Fig. 4c shows the comparison of the UV/vis absorption spectra of the pure ligand and of the Cu and Zn CPs. A significant bathochromic shift from 520 to >600 nm is observed, further confirming the formation of the coordination polymer, as will be detailed in the section below on modelling.[11,24] Fig. S7† shows the comparison of the UV/vis absorption spectra of the standard CP prepared from bulk solutions and the thin films prepared by shear coating, showing that there are no significant differences and that the shear processing does not damage the OHPTP ligands.

XRD measurements on the CPs revealed distinct crystalline structures arising from their different bonding configurations. After accounting for the crystalline substrate contributions, the XRD patterns in Fig. S9† show noticeable differences at lower angles, with a peak at 27.94° ± 0.03° for the Cu CP and a peak at 27.08° ± 0.07° for the Zn CP, corresponding to *d*-spacings of 3.19 Å and 3.29 Å, respectively. These peaks reflect the interlayer spacing of CPs. In the Zn CP, the presence of Zn ions forces a rotation and tilting of the ligands, causing a more pronounced distortion of the planar arrangement and thus a larger spacing. A qualitative estimate of the number of coherently scattering layers, derived from the peak width using the Scherrer equation, indicates 52 ± 1 MLs for the Cu CP and 26 ± 1 MLs for the Zn CP. The larger coherence length observed in the Cu-based system indicates that it is more crystalline than the Zn CP. This higher crystallinity likely stems from the more planar arrangement of the Cu CP.

Electronic properties of the Cu and Zn CPs

The work function (WF) of organic materials is a sensible indicator of their electronic properties and molecular assembling, and Kelvin probe force microscopy (KPFM) can be used to measure such WF on the nanometric scale, also on poorly conductive samples.[29–33]

In the case under study here, the WF of the sample will depend significantly on the interaction of ligands with each other and with the metal ions. KPFM measurements were performed with tips of known WF, calibrated on freshly cleaved HOPG and a gold reference substrate, and the results showed uniform values of WF for the samples, with no characteristic features, and a typical RMS variation for each measurement of 20 mV (Fig. S8†). Fig. 5 shows the comparison of the WFs of samples obtained with Cu and Zn, respectively, at different dipping times for a single cycle and for multiple dipping cycles.

Both films showed a decrease in the work function value with increasing dipping time, with the Zn CP film demonstrating the largest change, going from 5.05 ± 0.01 eV to 4.96 ± 0.01 eV after 20 min exposure to the Zn ion solution. Like many polyaromatic molecules, OHPTP can stack on top of each other and interact through their π orbitals (π–π stacking), and their electric properties depend strongly on the orientational order of the molecules in the film and their ability to form long stacks.

This significant decrease in the WF could thus be attributed to the disruption of the packing of the organic material, with a decrease of π–π interactions, again caused by a forced rotation and tilting of the ligands induced by Zn.

The shift in the WF with the number of reaction cycles showed a similar trend, even if more complex; the WF started to increase again after the 5th cycle, possibly due to partial dissolution and disruption of the thick, multi-layered CP.

Modelling of the material structure using DFT calculations

To better elucidate the structural, electronic, and optical properties of the Cu- and Zn-based coordination polymers having OHPTP units as ligands, we performed density functional theory (DFT) calculations on both single monomeric model complexes and on periodic 2D layers having different ion/ligand ratios.

It is worth noting that an ideal 2D monolayer of our metal–organic CPs would result in an ion/ligand ratio of 2 (Fig. 1b). Therefore, in such structures, the OHPTP ligand should not only fully deprotonate, but also partially oxidize,[11] resulting in an open-shell singlet diradical (Fig. S10†). DFT and TD-DFT calculations carried out on the pristine OHPTP single unit indicate that such a molecule should display a strong elec-

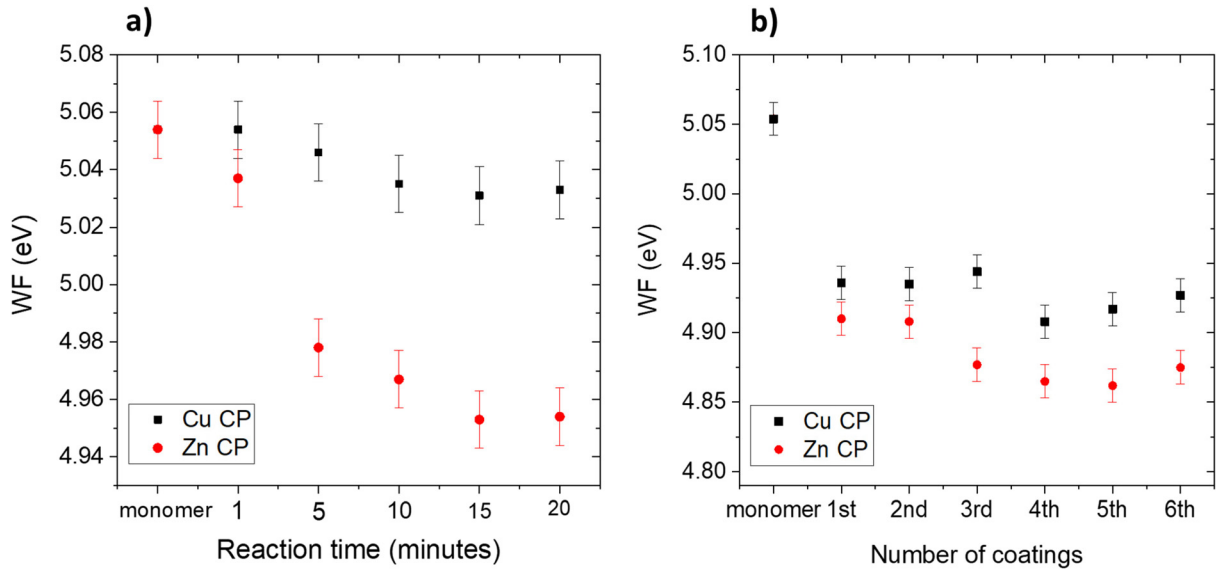

Fig. 5 Work function diagram with respect to (a) the reaction time and (b) the number of dipping cycles.

tronic transition at 319 nm (*i.e.*, $S_0 \rightarrow S_4$, having an oscillator strength of 1.30), with weak and low-energy absorption bands extending up to 365 nm (Table S1†). Accordingly, a very pronounced absorption feature at approx. 300–325 nm is observed in the experimental absorption spectrum of pristine OHPTP, but also a less pronounced broad and unstructured band is found in the 450–625 nm region (Fig. 4c). Such bands can be attributed to the partially oxidized forms of OHPTP, resulting in radicals featuring low-energy electronic transitions. Indeed, TD-DFT calculations carried out on the four-electron-oxidized forms of OHPTP (the actual species acting as ligands in the Cu and Zn CPs) show intense transitions at 448 and 602 nm (Fig. S11†), with a plethora of nearby less pronounced ones.

To provide a rationalization of the different reactivities of the copper(II) and zinc(II) ions in forming the corresponding metal–organic coordination polymers (see Table 1), 2D periodic DFT calculations were carried out to elucidate the structural modifications occurring in the OHPTP slab upon Cu^{2+} and Zn^{2+} complexation. The pristine OHPTP monolayer tends to form a zig-zag surface with fully planar OHPTP molecules, linked together by multiple hydrogen bonds and forming an angle of 71.2° between nearby molecular planes (Fig. 6a). Such 2D arrangement leads to a negligible conjugation between nearby OHPTP units (as shown by the flat band diagram in Fig. S12†), and the resulting band gap is wide (*i.e.*, 3.38 eV) since all ligands display a closed-shell configuration.

Upon partial oxidation, the 2D layer of four-electron-oxidized OHPTP molecules becomes virtually planar (Fig. 6b) and the related band structure displays wider bandwidths because of increased π conjugation between the ligands (Fig. S13†). Moreover, as already suggested by TD-DFT calculations performed on the individual OHPTP molecule, the band gap of this partially oxidized 2D organic network is strongly narrowed (*i.e.*, 1.28 eV) due to the di-radical nature of the OHPTP molecules. It should be emphasized that upon just deprotonation, this 2D surface can readily accommodate up to two M^{2+} ions per ligand.

The so-formed ideal 2D layers of Cu and Zn CPs display substantially different geometries in their fully relaxed minima. In the case of the Cu CP, the 2D metal–organic layer remains planar, preserving the same geometry of the four-electron-oxidized OHPTP monolayer (Fig. 6c); accordingly, due to modest rearrangements of the 2D network, a quick and efficient uptake of copper ions is expected by the partially oxidized ligand film, which can justify why high ion/ligand ratios are readily observed already after 1 minute of film dipping into a Cu^{2+}-rich solution, and the ideal ratio is almost reached after just 20 minutes (Table 1). In contrast, the formation of a Zn CP leads to a substantial deformation of the monolayer, leading to a zig-zag 2D network with nearby ligands being tilted by 57.9° (Fig. 6d); such remarkable structural changes upon zinc coordination can justify the inefficient uptake of Zn^{2+} ions by the free-ligand films, as experimentally observed (Table 1). Upon metal–organic CP formation, just a slight reduction in the band gap of these 2D networks is estimated (*i.e.*, 0.78 and 0.97 eV for the Cu and Zn CPs, respectively) since there is virtually no direct metal contribution to the highest valence band or the lowest conduction ones, as shown in Fig. S14 and S15.† Notably, despite a similar band gap, the band structures of these two CPs are radically different: in the case of the Cu CP, considerable band velocities are observed due to spin polarization effects exerted by the Cu^{2+} ions (having a d^9 configuration) and the flat surface of the related CP, inducing strong π conjugation; in contrast, the band structure of the Zn CP displays almost no band dispersion due to both the d^{10} closed-shell configuration of the Zn^{2+} ions and the zig-zag geometry of the layer.

The changes in the structural and electronic properties of the 2D monolayer of OHPTP molecules were further investi-

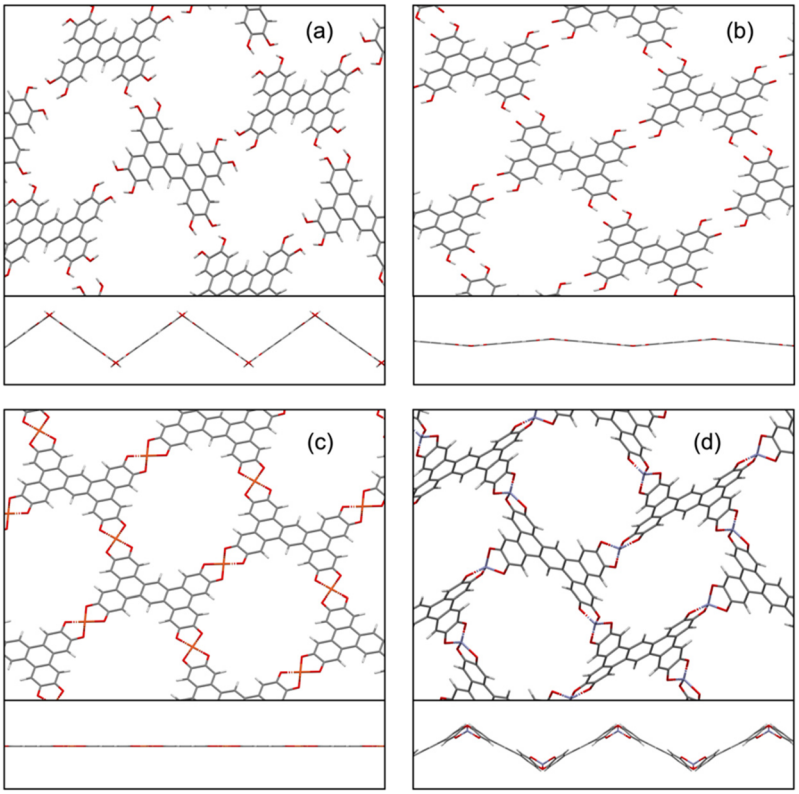

Fig. 6 Optimized structures of the ideal 2D monolayer of (a) the pristine OHPTP ligand, (b) the four-electron-oxidized OHPTP molecules, and the (c) Cu-based and (d) Zn-based coordination polymers. The lateral view of each monolayer is also provided.

gated, simulating also an intermediate uptake of metal ions (ion/ligand ratio of 1). As shown in Fig. S16,† the coordination of a fraction of Zn^{2+} ions to the partially oxidized OHPTP monolayer already leads to a remarkable perturbation of the ligand 2D network, passing from a nearly planar sheet to a zig-zag system with a tilting angle of 51.3°, being already very similar to the ideal (fully loaded) Zn CP (compare Fig. S15 and S18†). On the other hand, negligible changes are observed upon partial uptake of Cu^{2+} ions (*i.e.*, the 2D layer remains planar and the cell parameters are perturbed by less than 7%). Such theoretical findings can provide a qualitative justification of the remarkable changes in the WF of the Zn CP films, already observed at very short reaction times (*i.e.*, at very low Zn^{2+} loading, see Fig. 5a).

Electric charge transport at the nanometric scale

We performed electrical characterization of the single-coated Cu CP film produced with varying reaction times or coating cycles *via* conductive AFM (Fig. 7). The c-AFM technique can measure electric resistance in ultra-thin films, measuring the current passing across the film, from the substrate to the conductive tip, and is thus an ideal technique to measure the interaction due to π–π stacking of the molecules in the material. The conductance values were extracted from the corresponding current maps recorded *via* c-AFM averaging all points from each current map image.

Fig. 7a shows that a significant vertical conductance could be measured for all Cu CP samples, decreasing with reaction time, due to the uptake of ions. IR spectra were recorded at different reaction times (Fig. 4b) to confirm that there was no significant chemical change in OHPTP, with no uncontrolled reaction or degradation of the molecule upon time.

Conversely, the Zn CP samples prepared under the same conditions showed no conductance at all down to the instrument's sensitivity limit, suggesting again a significant decrease of π–π interactions and a disruption of the stacking upon metal ion coordination. We should underline that all Cu- and Zn-based samples had the same thickness, being deposited through shear coating, with the only varying parameter being the exposure time and the nature of the ionic solution. Thus, a dramatic disruption of electric properties could be caused by a smaller uptake of Zn ions (see Table 1) compared to the uptake of more compliant Cu ions.

The material thickness could be increased significantly by repeating the coating–ion exposure cycle multiple times (Fig. 7b). Conductance was also measured in-plane, *i.e.*, between two macroscopic electrodes, to study the anisotropic nature of the material (Fig. 7c, see the ESI† for experimental details). As could be expected, the in-plane conductance increased with an increase of the amount of the transporting material due to the presence of multiple conduction paths, reaching a constant value of ≈11 S m^{-1} already after three coat-

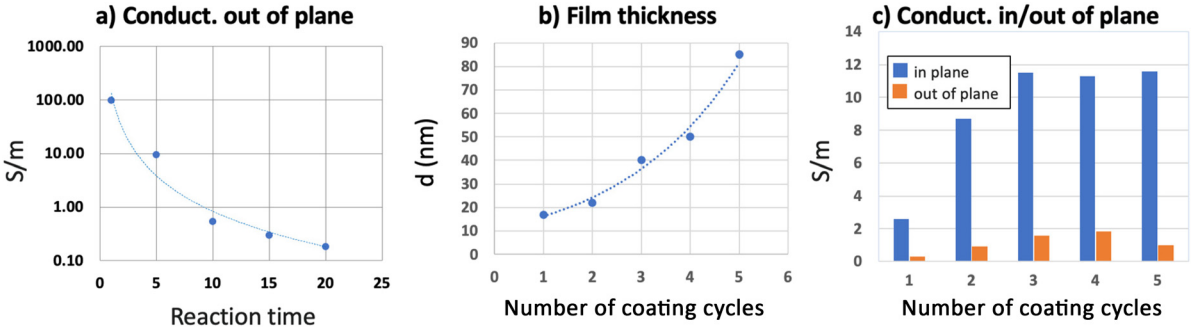

Fig. 7 (a) Conductance of the Cu CP measured out-of-plane (*i.e.* vertically) *vs.* the reaction time (exposure to the ionic solution). (b) Increase of Cu CP film thickness with the number of OHPTP coating steps. (c) Conductance of the Cu CP measured in-plane (*i.e.*, horizontally) and out-of-plane (*i.e.*, vertically) with increasing film thickness. The dotted lines are just a guide for the eye.

ings. The out-of-plane conductance increased as well going from 0.29 S m^{-1} after one coating to 1.82 S m^{-1} after four coatings, suggesting that layers deposited after the first layer are more ordered than the one deposited directly on the substrate. For further coatings, instead, the quality of the material decreased, showing lower conductance.

Stability of the CP thin films

Thermal stability studies were performed through temperature-controlled desorption using a residual gas analyzer (RGA) mounted inside a home-built XPS UHV chamber and (i) ramping up to 300 °C at a heating rate of 2 °C min^{-1} (slow desorption) or (ii) by flash heating for a few minutes up to 300 °C (fast desorption). Both desorption methods gave similar results, so only the samples prepared with the former will be discussed. Samples with a single coating, 1 min dipping time in Cu or Zn solutions, were measured by XPS prior and after the heating treatment to compare possible changes in their chemical composition due to thermal desorption.

Fig. 8a shows the Cu 2p signal of the Cu CP samples before and after heating. Initially, both the Cu(II) signal and Cu(I) signal are present, as expected. O 1s is also present and the carbon spectrum can be attributed to the carbonate or carboxyl acid groups. After heating at 300 °C (Fig. 8a, red line), the Cu signal completely disappeared, suggesting that the Cu was removed from the sample in the form of CuO. The presence of CuO in the gas produced during heating was then confirmed from the RGA data (Fig. S19 and S20†).

The Zn CP films showed instead much better stability than the Cu CP films, with no removal of Zn after heating, as indicated by XPS (Fig. 8b).

These findings are in general agreement with the thermal stability of many different MOFs, as reported in the literature.[34]

Both samples were also investigated using AFM and KPFM to detect any changes in their morphology or electrical properties linked to their thermal properties. Fig. 9 shows the morphology of both films prior and after their heat treatment. A moderate increase in the roughness of their surfaces can be detected, with the Cu samples showing also significant defects, with holes of ≈158 nm diameter likely due to the expulsion of gaseous products as indeed observed by RGA. No such damage was instead observed in Zn CP samples.

In agreement with the previous observation, the WF measured by KPFM also showed significant changes after the heating, in particular for Cu CP samples. The WF of Cu CP samples changed from 4.95 ± 0.02 eV to 5.07 ± 0.02 eV, likely due to significant damage due to gas expulsion. The Zn CP

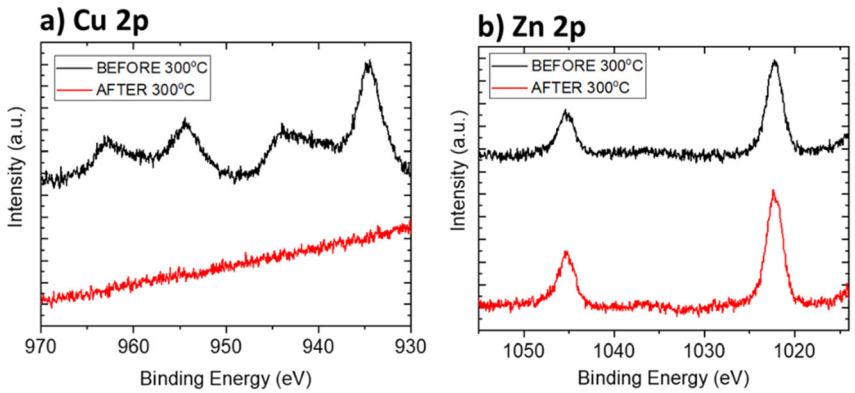

Fig. 8 Thermal stability of the single-coated Cu and Zn thin films. XPS spectra recorded prior to any heating and after heating at 300 °C in a vacuum for (a) the single-coated Cu thin film and (b) the single-coated Zn thin film.

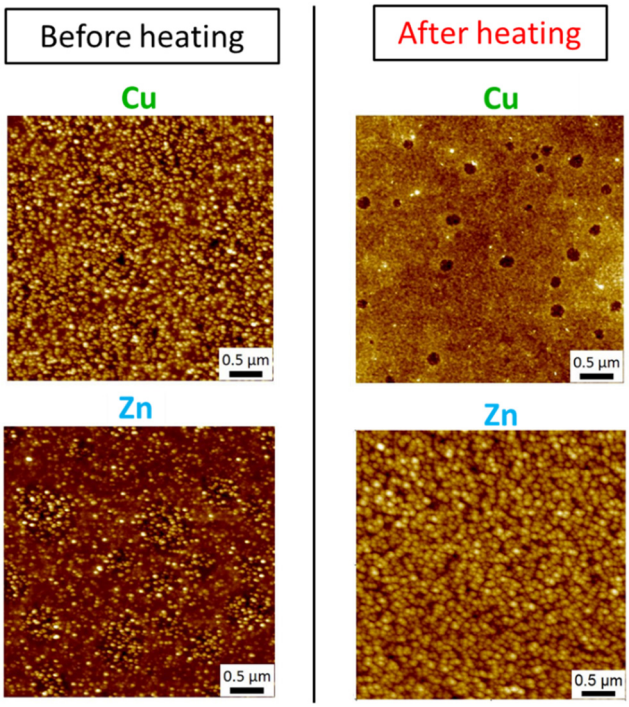

Fig. 9 AFM images of the CP films before and after heat treatment.

samples showed barely no change, going from 4.97 ± 0.02 eV to 4.96 ± 0.02 eV, in agreement with XPS results.

3. Conclusions

By combining complementary characterization techniques, we provided insight into the formation mechanism and structure–property relationship of coordination polymers (CPs) based on aromatic organic ligands, such as OHPTP, produced by a novel shear coating method; all data indicate that changing the binding ion from copper to zinc significantly alters the structure, electric properties, and thermal stability of the CPs, as summarized below.

FT-IR spectra confirm the presence of a coordination network, with the hydroxy groups of OHPTP reacting with the metal ions to different extents. The shear coating process, however, yields a CP that is less ordered than what is typically produced in the bulk from solutions.

XPS results show that when OHPTP is exposed to the solution of the metal ions during the reaction step, copper exhibits higher affinity for the ligand. It penetrates much faster into the organic film than zinc, reaching an atomic ratio of 1.6% already within just 1 minute (Table 1), and approaches the ideal stoichiometry after 20 minutes of reaction. On the other hand, zinc ions are present at a lower concentration in the material and never approach the ideal M_2(OHPTP) stoichiometry, achieving at best an ion/ligand ratio of 0.54. Given the similar size but different electronic configurations of the two ions, this result could be attributed to the better suitability of Cu to coordinate the organic molecules in a planar fashion, while the tendency of zinc to coordinate in a non-planar, tetrahedral geometry would require a stronger reorganization of the organic molecules. DFT calculations allow us to confirm and elucidate in detail this mechanism, showing that even partial uptake of Zn ions leads to a remarkable perturbation of the ligand 2D network, passing from a nearly planar sheet to a zigzag system with a tilting angle of 51.3°. Instead, Cu uptake causes negligible changes, with the 2D layer remaining planar and the cell parameters perturbed by <7%.

Consistently, the tilting observed in the Zn-based compound likely explains its larger interplanar spacing than that of the Cu-based compound observed by XRD.

The formation of CPs results in a lowering of the work function for both materials, with the Zn CP showing a more significant change. This could again be attributed to the forced disruption of the planar stacking and π–π interactions of OHPTP. This decrease in π–π interactions is also confirmed by C-AFM; in this case, the Cu CP shows only a partial decrease, while notably, the Zn CP films are completely insulating, suggesting again a more substantial disruption of the planar arrangement. This agrees with and confirms previous results that attribute the good electrical conductance of the Cu-based CP to the out-of-plane interactions of its stacked ligands. On a broader scale, it could also help to better clarify the crystal structure of 2D MOFs formed by Zn ions and catechol ligands, which has still not been elucidated at the atomic level and has been attributed to the tendency of Zn coordination complexes not to conform to classic planar tetragonal structures.[9]

Thermal annealing shows that the Cu CP, besides being easier to form, is also easier to disrupt, with the removal of Cu in the form of cuprous oxide, while the Zn CP is stable up to 300 °C.

Although more work is needed to reach a perfect understanding and achieve full control of the structures of these CPs at the molecular level, these results provide a solid starting point for identifying the key factors to obtain stable, highly ordered, and better-performing coordination polymers.

Data availability

The data supporting this article have been included as part of the ESI.†

Conflicts of interest

There are no conflicts to declare.

Acknowledgements

This work was financially supported by the H2020-MSCA-ITN ULTIMATE (grant number 813036) and the DFG project CRC-1415, No. 417590517.

References

1 S. Kitagawa, R. Kitaura and S. I. Noro, Functional Porous Coordination Polymers, *Angew. Chem., Int. Ed.*, 2004, 2334–2375, DOI: 10.1002/anie.200300610.

2 O. M. Yaghi, M. O'Keeffe, N. W. Ockwig, H. K. Chae, M. Eddaoudi and J. Kim, Reticular Synthesis and the Design of New Materials, *Nature*, 2003, **423**(6941), 705–714, DOI: 10.1038/nature01650.

3 X. M. Chen, Assembly Chemistry of Coordination Polymers, in *Modern Inorganic Synthetic Chemistry*, Elsevier, 2011, pp 207–225. DOI: 10.1016/B978-0-444-53599-3.10010-1.

4 C. H. Li and J. L. Zuo, Self-Healing Polymers Based on Coordination Bonds, *Adv. Mater.*, 2020, **32**(27), e1903762, DOI: 10.1002/adma.201903762.

5 S. R. Batten, Coordination Polymers, *Curr. Opin. Solid State Mater. Sci.*, 2001, **5**(2–3), 107–114, DOI: 10.1016/S1359-0286(00)00031-0.

6 S. R. Batten, N. R. Champness, X. M. Chen, J. Garcia-Martinez, S. Kitagawa, L. Öhrström, M. O'Keeffe, M. P. Suh and J. Reedijk, Terminology of Metal-Organic Frameworks and Coordination Polymers (IUPAC Recommendations 2013), *Pure Appl. Chem.*, 2013, **85**(8), 1715–1724, DOI: 10.1351/PAC-REC-12-11-20.

7 M. L. Foo, R. Matsuda and S. Kitagawa, Functional Hybrid Porous Coordination Polymers, *Chem. Mater.*, 2014, 310–322, DOI: 10.1021/cm402136z.

8 J.-P. Zhang, X.-C. Huang and X.-M. Chen, Supramolecular Isomerism in Coordination Polymers, *Chem. Soc. Rev.*, 2009, **38**(8), 2385, DOI: 10.1039/b900317g.

9 Y. Lu, P. Samorì and X. Feng, Rational Construction of Two-Dimensional Conjugated Metal–Organic Frameworks (2D c-MOFs) for Electronics and Beyond, *Acc. Chem. Res.*, 2024, **57**(14), 1985–1996, DOI: 10.1021/acs.accounts.4c00305.

10 E. R. Nightingale, Phenomenological Theory of Ion Solvation. Effective Radii of Hydrated Ions, *J. Phys. Chem.*, 1959, **63**(9), 1381–1387, DOI: 10.1021/j150579a011.

11 L. Sporrer, G. Zhou, M. Wang, V. Balos, S. Revuelta, K. Jastrzembski, M. Löffler, P. Petkov, T. Heine, A. Kuc, E. Cánovas, Z. Huang, X. Feng and R. Dong, Near IR Bandgap Semiconducting 2D Conjugated Metal-Organic Framework with Rhombic Lattice and High Mobility, *Angew. Chem., Int. Ed.*, 2023, **62**(25), e202300186, DOI: 10.1002/anie.202300186.

12 I. Hoeger, O. J. Rojas, K. Efimenko, O. D. Velev and S. S. Kelley, Ultrathin Film Coatings of Aligned Cellulose Nanocrystals from a Convective-Shear Assembly System and Their Surface Mechanical Properties, *Soft Matter*, 2011, **7**(5), 1957–1967, DOI: 10.1039/c0sm01113d.

13 C. Teixeira Da Rocha, G. Qu, X. Yang, R. Shivhare, M. Hambsch, Y. Diao and S. C. B. Mannsfeld, Mitigating Meniscus Instabilities in Solution-Sheared Polymer Films for Organic Field-Effect Transistors, *ACS Appl. Mater. Interfaces*, 2019, **11**(33), 30079–30088, DOI: 10.1021/acsami.9b07832.

14 Y. Diao, K. M. Lenn, W.-Y. Lee, M. A. Blood-Forsythe, J. Xu, Y. Mao, Y. Kim, J. A. Reinspach, S. Park, A. Aspuru-Guzik, G. Xue, P. Clancy, Z. Bao and S. C. B. Mannsfeld, Understanding Polymorphism in Organic Semiconductor Thin Films through Nanoconfinement, *J. Am. Chem. Soc.*, 2014, **136**(49), 17046–17057, DOI: 10.1021/ja507179d.

15 J. C. Lee, J. O. Kim, H. J. Lee, B. Shin and S. Park, Meniscus-Guided Control of Supersaturation for the Crystallization of High Quality Metal Organic Framework Thin Films, *Chem. Mater.*, 2019, **31**(18), 7377–7385, DOI: 10.1021/acs.chemmater.9b01996.

16 O. R. Juárez-Rivera, R. A. Mauricio-Sánchez, K. Järrendahl, H. Arwin and A. Mendoza-Galván, Shear-Coated Linear Birefringent and Chiral Cellulose Nanocrystal Films Prepared from Non-Sonicated Suspensions with Different Storage Time, *Nanomaterials*, 2021, **11**(9), 2239, DOI: 10.3390/nano11092239.

17 K. Haase, J. Zessin, K. Zoumboulis, M. Müller, M. Hambsch and S. C. B. Mannsfeld, Solution Shearing of a High-Capacitance Polymer Dielectric for Low-Voltage Organic Transistors, *Adv. Electron. Mater.*, 2019, **5**(6), 1900067, DOI: 10.1002/aelm.201900067.

18 K. Ditte, N. Kiriy, J. Perez, M. Hambsch, S. C. B. Mannsfeld, Y. Krupskaya, R. Maragani, B. Voit and F. Lissel, Charge Carrier Mobility Improvement in Diketopyrrolopyrrole Block–copolymers by Shear Coating, *Polymers*, 2021, **13**(9), 1435, DOI: 10.3390/polym13091435.

19 P. Dacha, M. Hambsch, D. Pohl, K. Haase, M. Löffler, T. Lan, X. Feng, B. Rellinghaus and S. C. B. Mannsfeld, Tailoring the Morphology of a Diketopyrrolopyrrole–based Polymer as Films or Wires for High–Performance OFETs Using Solution Shearing, *Small Methods*, 2023, **8**(3), 2300842, DOI: 10.1002/smtd.202300842.

20 I. Hoeger, O. J. Rojas, K. Efimenko, O. D. Velev and S. S. Kelley, Ultrathin Film Coatings of Aligned Cellulose Nanocrystals from a Convective-Shear Assembly System and Their Surface Mechanical Properties, *Soft Matter*, 2011, **7**(5), 1957–1967, DOI: 10.1039/c0sm01113d.

21 J. C. Lee, J. O. Kim, H. J. Lee, B. Shin and S. Park, Meniscus-Guided Control of Supersaturation for the Crystallization of High Quality Metal Organic Framework Thin Films, *Chem. Mater.*, 2019, **31**(18), 7377–7385, DOI: 10.1021/acs.chemmater.9b01996.

22 R. Li, S. Li, Q. Zhang, Y. Li and H. Wang, Layer-by-Layer Assembled Triphenylene-Based MOFs Films for Electrochromic Electrode, *Inorg. Chem. Commun.*, 2021, **123**, 108354, DOI: 10.1016/j.inoche.2020.108354.

23 Y. Lin, W. H. Li, Y. Wen, G. E. Wang, X. L. Ye and G. Xu, Layer-by-Layer Growth of Preferred-Oriented MOF Thin Film on Nanowire Array for High-Performance Chemiresistive Sensing, *Angew. Chem., Int. Ed.*, 2021, **60**(49), 25758–25761, DOI: 10.1002/anie.202111519.

24 W. Zhao, T. Chen, W. Wang, S. Bi, M. Jiang, K. Y. Zhang, S. Liu, W. Huang and Q. Zhao, Layer-by-Layer 2D Ultrathin Conductive Cu3(HHTP)2 Film for High-Performance Flexible Transparent Supercapacitors, *Adv. Mater. Interfaces*, 2021, **8**(11), 2100308, DOI: 10.1002/admi.202100308.

25 Z. Z. Ma, Q. H. Li, Z. Wang, Z. G. Gu and J. Zhang, Electrically Regulating Nonlinear Optical Limiting of Metal-Organic Framework Film, *Nat. Commun.*, 2022, **13**(1), 6347, DOI: **10.1038/s41467-022-34139-2**.

26 R. Zheng, Z. H. Fu, W. H. Deng, Y. Wen, A. Q. Wu, X. L. Ye and G. Xu, The Growth Mechanism of a Conductive MOF Thin Film in Spray-Based Layer-by-Layer Liquid Phase Epitaxy, *Angew. Chem., Int. Ed.*, 2022, **61**(43), e202212797, DOI: **10.1002/anie.202212797**.

27 M. Brust, P. M. Blass and A. J. Bard, *Self-Assembly of Photoluminescent Copper(I)-Dithiol Multilayer Thin Films and Bulk Materials*, 1997. **https://pubs.acs.org/sharingguidelines**.

28 W. M. Skinner, C. A. Prestidge and R. S. C. Smart, Irradiation Effects during XPS Studies of Cu(II) Activation of Zinc Sulphide, *Surf. Interface Anal.*, 1996, **24**(9), 620–626, DOI: **10.1002/(SICI)1096-9918(19960916)24:9<620::AID-SIA151>3.0.CO;2-Y**.

29 V. Palermo, M. Palma and P. Samori, Electronic Characterization of Organic Thin Films by Kelvin Probe Force Microscopy, *Adv. Mater.*, 2006, 145–164, DOI: **10.1002/adma.200501394**.

30 C. Musumeci, A. Liscio, V. Palermo and P. Samorì, Electronic Characterization of Supramolecular Materials at the Nanoscale by Conductive Atomic Force and Kelvin Probe Force Microscopies, *Mater. Today*, 2014, 504–517, DOI: **10.1016/j.mattod.2014.05.010**.

31 A. Liscio, E. Orgiu, J. M. Mativetsky, V. Palermo and P. Samorì, Bottom-up Fabricated Asymmetric Electrodes for Organic Electronics, *Adv. Mater.*, 2010, **22**(44), 5018–5023, DOI: **10.1002/adma.201002215**.

32 V. Palermo, G. Ridolfi, A. M. Talarico, L. Favaretto, G. Barbarella, N. Camaioni and P. Samorì, A Kelvin Probe Force Microscopy Study of the Photogeneration of Surface Charges in All-Thiophene Photovoltaic Blends, *Adv. Funct. Mater.*, 2007, **17**(3), 472–478, DOI: **10.1002/adfm.200600122**.

33 *Scanning Probe Microscopy*, ed. S. Kalinin and A. Gruverman, Springer New York, New York, NY, 2007. DOI: **10.1007/978-0-387-28668-6**.

34 C. Healy, K. M. Patil, B. H. Wilson, L. Hermanspahn, N. C. Harvey-Reid, B. I. Howard, C. Kleinjan, J. Kolien, F. Payet, S. G. Telfer, P. E. Kruger and T. D. Bennett, The Thermal Stability of Metal-Organic Frameworks, *Coord. Chem. Rev.*, 2020, **419**, 213388, DOI: **10.1016/j.ccr.2020.213388**.